

# Packed Bed Structure: Evaluation of Radial Particle Distribution

Néstor J. Mariani<sup>1,2</sup>, Wilson I. Salvat<sup>3</sup>, Osvaldo M. Martínez<sup>1,3</sup> and Guillermo F. Barreto<sup>1,3\*</sup>

<sup>1</sup> *Departamento de Ingeniería Química, Facultad de Ingeniería, Universidad Nacional de La Plata, La Plata, Argentina*

<sup>2</sup> *Pinmate, Departamento de Industrias, Facultad de Ciencias Exactas y Naturales, Universidad de Buenos Aires, Ciudad Universitaria, Buenos Aires, Argentina*

<sup>3</sup> *Centro de Investigación y Desarrollo en Procesos Catalíticos (CINDECA), CONICET- Universidad Nacional de La Plata, Calle 47 No. 257, CC 59, CP B1900AJK, La Plata, Argentina*

Packed beds contained in cylindrical vessels are widely applied in process industries, especially as fixed bed catalytic reactors. Fluid-dynamics and transport processes, particularly in multitubular beds exchanging heat with an external medium, are strongly influenced by the bed structure, which in turn is defined by the packing geometry and the ratio between the bed diameter and packing size, called the aspect ratio,  $a = d_T/d_p$ .

Radial structural properties have been studied from different points of view. In particular, radial voidage profiles have been experimentally evaluated in several studies (e.g., Ridway and Tarbuck, 1966; Benenatti and Brosilov, 1962; Goodling et al., 1983; Mueller, 1992). For spherical or round particles, the radial voidage changes from exactly one at the vessel wall to an asymptotic value in the bulk of the bed in the manner of a damped wave. This variation is explained by the fact that the vessel wall prevents particles from being randomly distributed close to it and causes the formation of an adjacent particle layer. In turn, this first layer induces the building of a less neatly defined second layer and so on.

In order to obtain a quantitative description of radial voidage variations, some alternatives have been employed (Mariani et al., 1998). The approach most frequently used is to advance an empirical function and adjust some fitting parameters by regression of experimental data.

An alternative approach is to develop a model to describe the radial distribution of particle centres (Govindarao and Froment, 1986; Mariani et al., 1998). The distribution is also evaluated from experimental information. This approach allows the evaluation of radial voidage profiles, but in addition, it intrinsically provides the identification of the particle layers nearest to the vessel wall, from which a discrete model for the solid phase in packed beds can be formulated.

The aim of this work is to reach a satisfactory description of the packed bed structure in the region close to the vessel wall for the case of uniform spherical packing. The region extending from the wall up to one particle diameter (i.e., that corresponding to the first particle layer) is considered critical with respect to aspects such as channelling

A model describing the radial distribution of monosized spheres in randomly packed beds up to distances of about two particle diameters from the vessel wall is presented here. The model is based on the existence of a highly ordered layer of particles adjacent to the wall followed by a more diffuse, but still identifiable, second layer. Expressions generated from simple geometrical concepts (intersection between a cylindrical surface and a sphere) straightforwardly allow calculating the radial voidage profile given the radial distribution of particle centers and vice versa. These expressions are employed to fit the model to measures of voidage profiles within a wide range of aspect ratios,  $a = (R_T/R_p)$ . The model can be used to accurately predict radial voidage profiles, but it is stressed that the identification of particle distribution constitutes more valuable information than an empirical expression for describing voidage variations.

On présente ici un modèle décrivant la distribution radiale de sphères monodisperses dans des lits garnis aléatoires jusqu'à des distances d'environ deux diamètres de particules de la paroi du réservoir. Le modèle s'appuie sur l'existence d'une couche très ordonnée de particules adjacentes à la paroi, suivie d'une seconde couche, plus diffuse mais cependant identifiable. Les expressions provenant de concepts géométriques simples (intersection entre une surface cylindrique et une sphère) permettent de calculer directement le profil de vide radial lorsque la distribution radiale des centres de particules est donnée et vice versa. Ces expressions servent à caler le modèle de mesures de profils de vide dans une vaste gamme de paramètres d'élanement,  $a = (R_T/R_p)$ . Le modèle peut être utile pour prédire de manière précise les profils de vide radiaux, mais il faut dire que la détermination de la distribution des particules constitue une information plus valable qu'une expression empirique pour décrire les variations de vide.

**Keywords:** bed structure, particle center distribution, voidage profile, aspect ratio.

\*Author to whom correspondence may be addressed. E-mail address: barreto@quimica.unlp.edu.ar

(Winterberg et al., 2000) or heat transfer toward the wall (Legawiec and Ziolkowski, 1994). Thus, attending to these practical conclusions, we will restrain the detailed description up to distances of about 2 to 2.5 particle diameters from the wall (the region covered by the first two layers).

For this purpose, a model in which the bed is divided into zones identified by the number of particle centres lying on them will be developed. The model incorporates the experimental evidence presented by Legawiec and Ziolkowski (1994) concerning the particle layer adjacent to the wall. In addition, experimental voidage profiles from different sources covering a wide range of aspect ratios will be considered for adjusting the model parameters.

Both fitting the model to the experimental data and for using the model as a predictive tool for the radial voidage profile, a mathematical relationship between a distribution of particle centres and the voidage profile is required. This relationship has been recently presented (Mariani et al., 2001) in terms of elliptic integrals, avoiding the use of numerical integration and accounting exactly for curvature effects.

### A Model for the Distribution of Particle Centres

Considering a packed bed long enough to neglect end effects, the radial density function of particle centres  $\rho(r_c)$  is defined so that  $[2\pi\rho(r_c)r_c dr_c]$  accounts for the number of particle centres per unit bed length in a cylinder of radius  $r_c$  and thickness  $dr_c$ . Recalling that in randomly packed beds, particles are accommodated from the vessel wall as a series of layers with a decreasing degree of order, the density function  $\rho(r_c)$  can be conceived as built up from the contributions of a series of zones of high concentration of particle centres separated by spaces of negligible concentration. The first zone, corresponding to particles with their centres tight [to a distance  $(1/2)d_p$ ] to the wall, will show the highest density of particle centres and a very thin width. The second zone will be confined to a distance of about  $(3/2)d_p$ , but it will be thicker and have a lower particle centre density than the first layer. This trend is maintained toward the interior of the bed. If the aspect ratio is high enough, a point is reached in which the zones overlap (i.e., no space in between is left), defining an innermost, fully randomized region extending up to the bed axis. This region can be considered as the last zone, with uniform density of particle centres. From this description, it is better to write down  $\rho(r_c)$  as the sum of the zone contributions rather than as a continuous function:

$$\rho(r_c) = \sum_{j=1}^M \rho_j(r_c) \quad (1)$$

In order to define the zone density function  $\rho_j(r_c)$  and the number of zones,  $M$ , some conclusions from previous investigations are used. Legawiec and Ziolkowski (1994) measured the position of particle centres located in a region extending up to approximately  $1d_p$  from the vessel wall. To perform these measures, the authors generated a consolidated bed from the solidification of a polymer solution in its voids, which could be extracted from the vessel.

The visible structure adjacent to the wall allowed them to count the number of particles in effective contact with it. In addition, they used a depth gauge to verify the non-existence of separation between these particles and the vessel wall. For the more internal spheres, the experimental procedure consisted of

drilling through the polymer to a sphere surface. Then, the depth gauge was introduced into the orifice to measure the gap between the sphere surface and the vessel wall. In this way, the spheres close to the wall were classified in three groups:

- Group A: spheres whose centres are exactly at  $0.5d_p$  from the wall (in effective contact with it).
- Group B: spheres whose centres are in an interval  $0.9$  to  $1d_p$  from the wall.
- Group C: spheres whose centres are in an interval  $1$  to  $1.1d_p$  from the wall.

Particles were not detected out of the intervals indicated, i.e., between  $0.5$  to  $0.9d_p$ .

Most of the spheres were those belonging to Group A, amounting 90.4%. Only 1.1% of the spheres classified as Group B, while a more significant percentage, 8.5%, was counted for Group C.

Two significant conclusions arise from these results. First of all, a high concentration of particle centres exists at a distance of  $0.5d_p$  from the wall. They can be regarded as those particles comprising a first particle layer in contact with the wall. This fact will be incorporated in the proposed model by considering that the first zone of particle centres is defined by a density function,  $\rho_1(r_c)$ , equaling an impulse function concentrated at  $0.5d_p$  from the vessel wall.

On the other hand, the existence of Group B and C particles is justified by failures in the array of particles in contact with the wall, causing holes in which Group B and C particles can fit. Since Group B particles are scarce, in order to simplify the model we will lump both groups into a second zone that extends from  $1d_p$  to  $1.1d_p$  with a uniform density function  $\rho_2(r_c)$ . The particles in this zone will make up 9.6% of the total number in both the first and second zones.

The identification of the second particle layer (third zone of the model) is more difficult since, as described above, the effect of the wall becomes weaker towards the bed axis. Thus, we can expect that the particle centres extend over a finite region rather than being concentrated at a point as in the first layer, but the position and thickness of the third zone can not be quantified beforehand. Consequently, the third zone of the model will be defined as presenting a finite thickness (to be evaluated) and a uniform density function  $\rho_3(r_c)$ .

Particle centres beyond the third zone and up to the bed axis will be assumed to be uniformly distributed in a fourth zone. The thickness of the separation gap between the third and fourth zones will be also regarded as a parameter to be adjusted from experimental evidence.

According to the outlined model, Equation (1) becomes:

$$\rho(r_c) = \sum_{j=1}^4 \rho_j(r_c) \quad (2)$$

with

$$\rho_1(r_c) = \delta(r_c, R_T - R_p) N_{p1} \quad (3a)$$

$$\rho_j(r_c) \begin{cases} \bar{\rho}_j & \text{if } r_c \in (r_j^i, r_j^e) \\ 0 & \text{if } r_c \notin (r_j^i, r_j^e) \end{cases}; \quad \bar{\rho}_j = \frac{N_{pj}}{\pi[(r_j^i)^2 - (r_j^e)^2]}; \quad j = 2, 3, 4 \quad (3a)$$

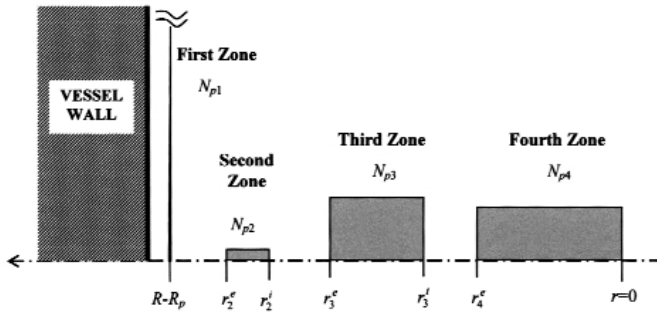


Figure 1. Sketch of zones for defining the function  $\rho(r)$ .

where  $N_{pj}$  is the number of particle centres per unit bed length in the  $j^{\text{th}}$  zone,  $r_j^i$  and  $r_j^e$  are the internal and external radii of the  $j^{\text{th}}$  zone and the impulse function is normalized according to:

$$2\pi \int_0^{R_T} \delta(r_c, r_j) r_c dr_c = 1 \quad (4a)$$

The values  $r_j$  can be re-expressed as follows:

$$r_j^i = R_T - 2R_p x_j^i; \quad r_j^e = R_T - 2R_p x_j^e \quad (4b)$$

where  $x_j$  is the dimensionless distance from the wall in units of  $d_p$ . A sketch of the proposed model for the distribution of particle centres is shown in Figure 1.

Table 1. Expressions for  $S(\xi, \mu)$  (Mriani et al., 2001).

Trivial cases

$$\mu \geq (R_p + \xi) \text{ (sphere outside cylinder):} \quad S/\xi = 0; \quad V = 0$$

$$\mu \leq (R_p - \xi) \text{ (sphere inside cylinder):} \quad S/\xi = 0; \quad V = (4/3)\pi R_p^3$$

$$\mu = \xi = 0 \quad S/\xi = 4\pi R_p^2; \quad V = 0$$

Degenerated case,  $(\xi + \mu) = R_p$

$$S/\xi = 16(\mu\xi)^{1/2}; \quad V = \frac{4}{3} \left[ R_p^3 \arccos\left(\frac{\mu - \xi}{R_p}\right) - 2(\mu\xi)^{1/2} \left( \frac{8}{3} \mu\xi + \mu^2 - \xi^2 \right) \right]$$

General case:  $|\mu - \xi| < R_p; \xi + \mu \neq R_p; \xi + \mu \neq 0$

$$\frac{S}{\xi} = 8R_p \omega \left[ (1 - \phi_B)F - \frac{1}{3}(\phi_A - \phi_B)D \right]$$

$$V = \frac{4}{3} R_p^3 \left\{ \theta + \omega \left[ \left( \alpha + \beta\phi_B + \frac{\Delta}{\phi_A} \right) F + \frac{1}{3}(\phi_A - \phi_B)(\tilde{z}_j + \beta D) \right] \right\}$$

where

$$\phi_B = \left( \frac{\mu - \xi}{R_p} \right)^2, \quad \phi_S = \left( \frac{\mu + \xi}{R_p} \right)^2, \quad \phi_A = \min(1, \phi_S), \quad \phi_M = \max(1, \phi_S), \quad \omega = (\phi_M - \phi_B)^{-1/2}$$

$$F = R_F(0, k^2, 1); \quad D = R_D(0, k^2, 1) \quad k^2 \frac{\phi_M - \phi_A}{\phi_M - \phi_B}$$

and (just for V)

$$\theta = \begin{cases} \pi & \text{if } \mu < \xi \\ \pi/2 & \text{if } \mu = \xi \\ 0 & \text{if } \mu > \xi \end{cases}, \quad \Delta = \frac{\mu^2 - \xi^2}{R_p^2}, \quad \alpha = \frac{1}{3}(\phi_B + \phi_S + \Delta^2 - 6\Delta - 3); \quad \beta = \frac{1}{3}[4 + 3\Delta - 2\Delta(\phi_B + \phi_S)];$$

$$\tilde{z}_j = \begin{cases} \frac{\Delta}{\phi_A^2} k^2 R_j \left( 0, k^2, 1, k^2 \frac{\phi_B}{\phi_A} \right), & \text{if } \Delta \neq 0 \\ 0 & \text{if } \Delta = 0 \end{cases}$$

The parameters to be adjusted are: the number of particle centres per unit bed length in the first and the third zones,  $N_{p1}$  and  $N_{p3}$ , the internal and external radii of the third zone, or, according to Equation (4),  $x_3^i$  and  $x_3^e$ , and the distance  $x_4^e$  for the fourth zone.

For the second zone, according to the assumptions discussed above,  $N_{p2} = 0.106N_{p1}$ ,  $x_2^i = 1.1$  and  $x_2^e = 1$ . Finally, the number of particle centres in the fourth zone  $N_{p4}$  is evaluated from the total number of particles in the bed  $N_{p'}$  which should satisfy:

$$N_p = \sum_{j=1}^4 N_{pj} \quad (5)$$

$N_p$  can be expressed in terms of the average bed voidage  $\bar{\epsilon}$ :

$$N_p = \frac{3}{2}(1-\bar{\epsilon})\frac{d_T^2}{d_p^3} = \frac{3}{2}(1-\bar{\epsilon})\frac{\alpha^2}{d_p} \quad (6)$$

Values of  $\bar{\epsilon}$  are calculated in this work from the experimental data used for fitting the parameters. By contrast, when using the model for predictive purposes, the following expression based on that suggested by Mariani et al. (1998) can be used to evaluate  $\bar{\epsilon}$  as a function of the aspect ratio:

$$\bar{\epsilon} = 0.375 + \frac{0.355}{a}$$

## Relationship between Voidage Profile and Particle Centre Distribution

The local voidage  $\epsilon(r)$  is defined as the fraction of voids intersected by a cylindrical surface of radius  $r$ . For monosize spheres,  $\epsilon(r)$  is related to  $\rho(r_c)$  as follows (Mariani et al., 2001):

$$\epsilon(r) = 1 - \int_0^{R_T} \frac{S(r, r_c)}{r} \rho(r_c) r_c dr_c \quad (7)$$

where  $S(\xi, \mu)$  is the area of a cylindrical surface of radius  $\xi$  intersected by a sphere of radius  $R_p$  centred at a distance  $\mu$  from the cylinder axis.

Replacing  $\rho(r_c)$  from Equation (2) into Equation (7) and accounting for the definitions given by Equations (3a, b), the procedure developed by Mariani et al. (2001) yields:

$$\epsilon(r) = 1 - \left\{ N_{p1} \frac{S(r, R_T - R_p)}{2\pi r} + \sum_{j=2}^4 \bar{\rho}_j \left[ V(r_j^e, r) - V(r_j^i, r) \right] \right\} \quad (8)$$

where  $V(\xi, \mu)$  is the volume of a sphere of radius  $R_p$  left inside a cylinder of radius  $\xi$ . Again, the distance from the sphere centre to the cylinder axis is  $\mu$ .

The geometrical quantities  $S(\xi, \mu)$  and  $V(\xi, \mu)$  are calculated by using the expressions displayed in Table 1 (Mariani et al., 2001), where  $R_r$ ,  $R_D$  and  $R_j$  are the Carlson's elliptic integrals of the 1<sup>st</sup>, 2<sup>nd</sup> and 3<sup>rd</sup> kind respectively (Press et al., 1992).

## Adjusting the Model Parameters from Experimental Information

Several experimental techniques have been used to evaluate radial voidage profiles in packed beds. A review of the subject can be found in Mariani et al. (1998). An analysis of available experimental data in their bibliography allowed some unreliable

**Table 2.** Experimental data used for the fitting procedure.

$a$	$\bar{\epsilon}$	Authors
5.60	0.438	Benenatti and Brosilow (1962)
7.62	0.422	Ridgeway and Tarbuck (1966)
8.56	0.417	Goodling et al. (1983)
10.70	0.408	Goodling et al. (1983)
14.10	0.400	Benenatti and Brosilow (1962)
20.30	0.392	Benenatti and Brosilow (1962)
$\infty$	0.378	Benenatti and Brosilow (1962)

**Table 3.** Values of fitted parameters.

Parameter	$x_3^e$	$x_3^i$	$x_4^e$	$x_w$	$G_1$	$G_3$
Value	1.209	1.486	1.735	0.894	0.825	0.710

data to be discarded. Accordingly, radial voidage profiles with the following features were discarded as unreliable:

1. Those not showing the typical damped wave from the vessel wall to the axis; and
2. Where the extrema along the wave show atypical values.

The sources of experimental radial profiles finally selected, along with aspect ratios and average voidages, are shown in Table 2. It must be pointed out that these data involve a wide range of aspect ratios.

A FORTRAN code (Greg Software Package) developed by Stewart et al. (1992) was used to fit the experimental radial profiles to Equation (8).

The fitted values of the dimensionless distances,  $x_3^i$ ,  $x_3^e$  and  $x_4^e$ , which define the locations of the third and fourth zones, are shown in Table 3. No significant trend between these parameters and the aspect ratio was found.

By contrast, the number of particles in the first and third zones  $N_{p1}$  and  $N_{p3}$  (the remaining fitting parameters) showed a dependence on the aspect ratio. In order to correlate this behaviour, we have considered compact arrangements that can be envisaged for a layer of particles accommodated against the vessel wall. There are at least two ways of establishing compact arrangements. The first, a 'crown' arrangement, is defined by adding particles in contact with one another around the internal perimeter of the tube. The next crown of spheres is built in the same way, allowing each particle to rest in the cavity formed by each pair of particles in the preceding crown, and so on. The second alternative, a 'string' arrangement, is obtained by placing one particle on top of another along the bed height, forming a string of particles. The next string is built by lodging each succeeding particle in the holes left in the former string. The number of particles in a crown or the number of even strings turns out to be a whole number only for some specific values of  $a$ . For instance, just two strings fit in the tube if  $a = 1.866$ , four for  $a = 2.22$  and so on. The crown arrangement can be used from a minimum value  $a = 2$ , when a crown is formed by two spheres. Nonetheless, for our purposes the number of particles per unit bed length,  $N_c$ , resulting from either arrangement, will be regarded as a continuous function of  $a$ .

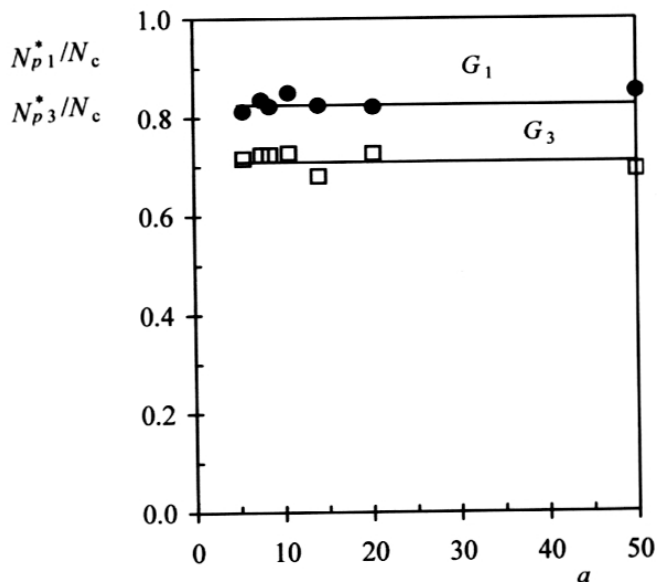


**Figure 2.** Fitting of the model parameters: ● Optimum  $N_{p1}^*/N_c$  values for each  $a$ ; □ Optimum  $N_{p3}^*/N_c$  values for each  $a$ ; — Optimum  $G_1$  and  $G_3$  values (Equations 10, 11).

It has been proven that values of  $N_c$  for both arrangements are almost indistinguishable if  $a > 2.2$ . As the minimum  $a$  employed here for the fitting procedure is  $a = 5.6$ , no difference is actually found. Adopting the expression for the string arrangement:

$$N_c(a) = \frac{\pi}{\beta d_p} \quad (9)$$

$$\text{where } \beta = \arcsin \left[ \frac{\left(\frac{3}{4}\right)^{1/2}}{a-1} \right]$$

Taking Equation (9) into account, we have expressed the number of particles in the first zone of our model by:

$$N_{p1} = G_1 N_c(a) \quad (10)$$

where  $G_1$  is a parameter considered independent of  $a$ .

For  $N_{p3}$ , an analogous expression can be written by considering a 'fictitious wall' at a dimensionless distance  $x_w$  from the vessel wall. The aspect ratio for the bed thus defined results:

$$a' = a - 2x_w \quad (11)$$

where  $G_3$  is a parameter, which is also assumed independent of  $a$ .

In summary, the parameters to be fitted for the range of aspect ratios here analysed are:  $x_w$ ,  $G_1$  and  $G_3$ . The best-fit values are presented in Table 3.

Best values of  $N_{p1}^*$  and  $N_{p3}^*$  were also obtained for each experimental voidage profile to check if the ratios  $N_{p1}^*/N_c$  and  $N_{p3}^*/N_c$  can be effectively considered as being independent of  $a$ . The comparison between,  $N_{p1}^*/N_c$ ,  $N_{p3}^*/N_c$  and  $G_1$ ,  $G_3$  is

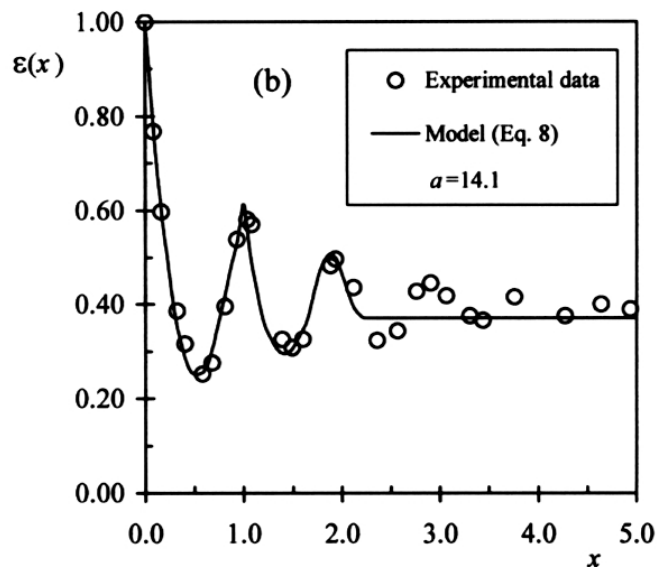
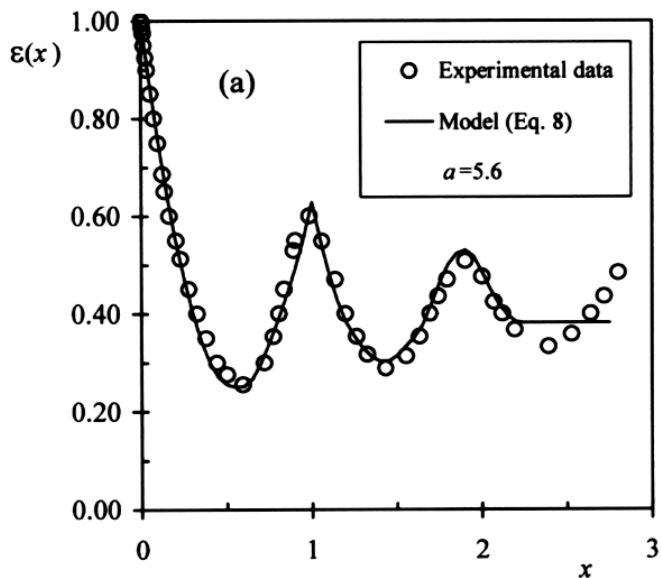


**Figure 3.** Comparison between experimental and predicted radial voidage profiles (Equation 8): (a) at  $a = 5.6$  (Benenatti and Brosilow, 1962); (b) at  $a = 14.1$  (Benenatti and Brosilow, 1962).

displayed in Figure 2. It can be clearly appreciated that the ratios  $N_{p1}^*/N_c$  and  $N_{p3}^*/N_c$  show no definite trend in the studied range of  $a$ , and their dispersion is satisfactorily low. The values obtained for  $G_1$  and  $G_3$  indicate that both the first and second particle layers are more loosely packed than in a compact theoretical arrangement. As expected, the second layer deviates more strongly than the first one.

The quality of the fit can be appreciated in Figures 3a, b for  $a = 5.6$ , and  $a = 14.1$  and in Figure 4 for  $a = 20.3$ . The model fits the experimental curves in a very satisfactory way, from the wall up to  $x \cong 2.2$ , the region where the voidage profile is dominated by the two first particle layers included in the model. Two stationary minima and two stationary maxima appear in this region. The values of voidage and positions of these

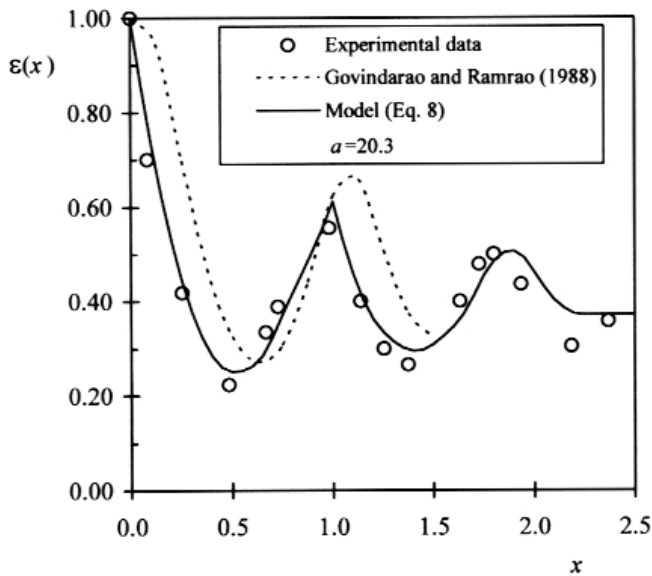


**Figure 4.** Comparison between experimental radial voidage profile at  $a = 20.3$  (Benenatti and Brosilow, 1962) and values predicted by the present model (Equation 8) and from Govindarao and Ramrao (1988).

extrema are particularly well reproduced by the model. The overall error for all fitted experimental voidage profiles, expressed as the average of absolute values,  $(\epsilon_{exp} - \epsilon_{calc})/\epsilon_{exp}$  is about 7%.

Two sets of experimental values not included in the fitting procedure are those presented by Mueller (1992) at  $a = 5.96$ , and by Giese et al. (1998) at  $a = 9.3$ . A very good agreement is found between model predictions and these data, as shown in Figures 5 a, b.

As noted above, the region from the vessel wall up to one particle diameter is critical as far as local bed transport properties and local permeability are concerned. The results from the model are particularly precise in this region and some points are worth remarking:

- The effect of the vessel curvature on the position of the first minimum voidage is correctly predicted. A close inspection of experimental voidage profiles shows that the position of the first minimum voidage moves farther from the wall as  $a$  decreases, as revealed by the data collected by Mariani et al. (1998). At large values of  $a$ , the first minimum corresponds to  $x_{min} = 0.5$ , i.e., the position of the centre of a particle touching the wall. At any value of  $a$ , the minimum voidage location predicted by the model can be found by minimizing the values from Equation (8), considering that only the first two zones will contribute in the region close to  $x = 0.5$ . The results thus obtained are in good agreement with the experimental data. The values of  $x_{min}$  can also be precisely approximated, at least for  $a > 4$ , by the following expression:

$$x_{min} = 0.5 \left\{ 0.9a - \left[ (0.9a - 1)^2 - 1 \right]^{0.5} \right\} \quad (12)$$

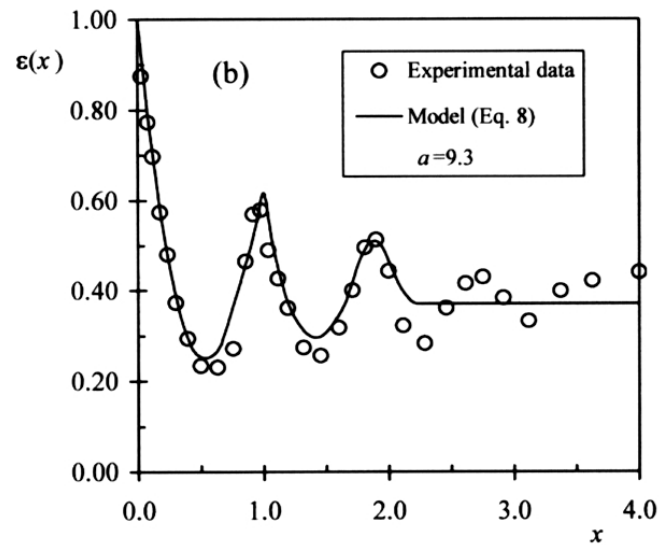
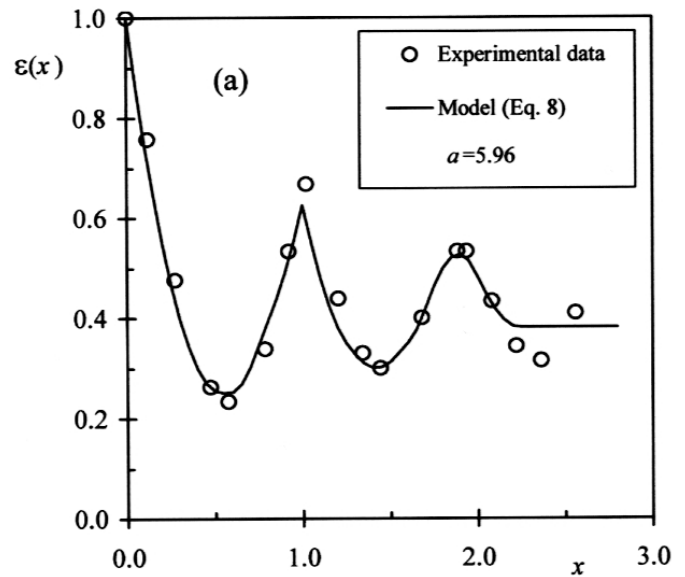


**Figure 5.** Comparison between experimental and predicted radial voidage profiles (Equation 8): (a) at  $a = 5.96$  (Mueller, 1992); (b) at  $a = 9.3$  (Giese et al., 1998).

- The model predicts a maximum slope of the voidage profile at the vessel wall. At least within the precision allowed by the discrete number of data points reported in experimental work, the slope of the voidage profile is maximum at the vessel wall. This effect can be appreciated in Figures 3, 4 and 5. These figures also show that the model yields a maximum slope at the wall. This property can only be achieved if  $\rho_1(r_c)$  is defined as an impulse function. By contrast, if a step function is assumed for  $\rho_1(r_c)$  (as for the remaining zones), the slope at  $x = 0$  will be exactly zero, and an inflection point will appear closer to the wall, indicating a thinner first zone.

The effect of the first zone size can be visualized from the pioneer model for particle centre distribution developed by Govindarao and Froment (1986). The bed is divided into zones of equal thickness  $(1/6)d_p$ , with some zones devoid of particles centres

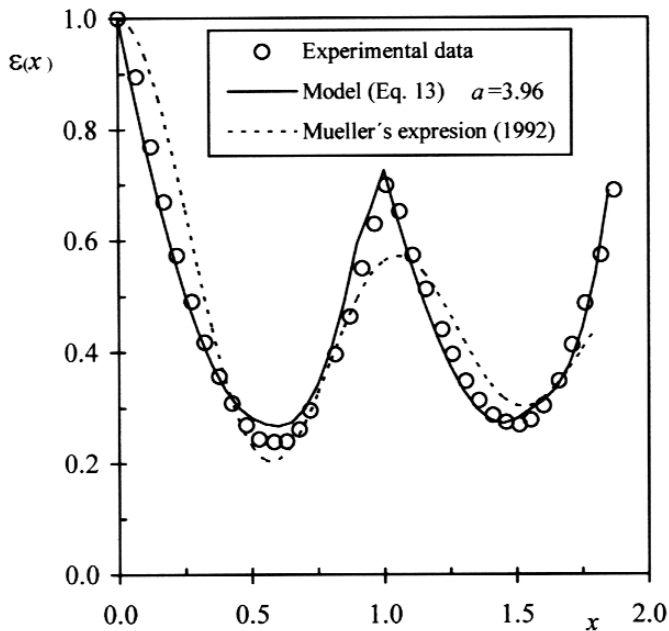


**Figure 6.** Comparison between experimental (Mueller, 1992) and predicted radial voidage profile (Equation 13) at  $a = 3.96$ .

and others filled in by particle centres with uniform density. The first zone, as in the model presented here, represents the first particle layer and extends from  $x = 0.5$  to  $x = (2/3)$ . Values of  $N_{p1}$  for this model were correlated later with  $a$  by Delmas and Froment (1988) and, independently, by Govindarao and Ramrao (1988). The profile predicted from the model for  $a = 20.3$ , according to results obtained by Govindarao and Ramrao (1988), has been plotted in Figure 4, where the shape of the curve close to the wall produced by the finite thickness of the first zone is clearly revealed.

### Extension to Lower Aspect Ratios

The lowest  $a$  included in the set of experimental data employed in the fitting of model parameters is  $a = 5.6$ , so the use of values reported in the previous section should be constrained within this lower bound.

Although it is not common to find industrial multitubular packed beds with aspect ratios  $a < 5.6$ , the interest of such cases cannot be ignored, as for pilot plant applications. The range  $1 < a \leq 2$  is very specific in the sense that stable particle positions can be conceived only if they touch the wall. This fact has been treated quantitatively by Govindarao et al. (1992), who developed an analytical expression to evaluate  $N_{p'}$ , which was successfully validated against experimental evidence. In terms of the model presented here, the first zone encompasses the whole bed with  $N_{p1} = N_p$ . The use of Equation (8), reduced to  $\varepsilon(r) = 1 - N_{p1} S(r, R_T - R_p) / (2\pi r)$ , was suggested by Mariani et al. (2000).

To our knowledge, there is little experimental information in the remaining range  $2 < a < 5.6$ . We consider here the experimental results for local voidages reported by Mueller (1992) for  $a = 3.96$ , which are plotted in Figure 6, along with predicted values from an empirical correlation proposed by the author. If we employ the approach presented here for this aspect ratio, it must be noted that the fourth zone loses its

meaning because its thickness becomes almost negligible ( $0.14d_p$ ), with the value  $x_4^e$  in Table 3. On the other hand, the shape of the experimental profile indicates that the fraction of solid in the bed centre region is very small. The fourth zone is then removed, as a first approximation. We perform the regression of these data to get a specific set of best-fit parameters. It turns out that the third zone is better modelled by an impulse function, rather than by a step function, for  $\rho_3(r_c)$ . Then, Equation (8) becomes:

$$\varepsilon(r) = 1 - \left\{ N_{p1} \frac{S(r, R_T - R_p)}{2\pi r} + \bar{\rho}_2 [V(r_2^e, r) - V(r_2^i, r)] + N_{p3} \frac{S(r, r_3)}{2\pi r} \right\} \quad (13)$$

The fitted values were  $G_1 = 0.801$ ,  $x_3 = 1.411$  (the location of the second pulse), and  $G_3 = 0.765$  calculated from Equation (11), with  $a' = a - 2(x_3 - 0.5)$ . A very good match with the experimental results is obtained in this way (Figure 6).

The values of  $G_1$  and  $G_3$  and the negligible thickness of the third zone suggest that the first and second particle layers exhibit a much closer resemblance for  $a = 3.96$  than for  $a > 5.6$ . In particular, the second zone has become more compact and well ordered. This effect is likely produced by the size of the tube, which very approximately allows the formation of just two particle layers, thus impairing the dispersion of second-layer particles.

It can be concluded that the approach followed in this study is likely to be useful for low aspect ratios in the range  $2 < a < 5.6$ , while very strong geometrical constraints within this range may introduce configurations highly depart on the aspect ratio, which in turn will be reflected by the values of the model parameters.

### Conclusions

A model capable of describing the structure of a cylindrical packed bed of monosized spheres has been presented in this work. It is based on evaluating the density number of particle centres along the tube radius. The model represents a better alternative than traditional empirical correlations for estimating radial voidage variations in the region close to the vessel wall. Voidage profiles can be precisely described and at the same time, the first and the second particle layers adjacent to the wall can be identified. The latter information is essential for modelling packed beds from a discrete point of view, i.e., by acknowledging the discontinuous nature of the solid phase. This kind of model is likely to provide a better support for interpreting and correlating bed properties close to the vessel than pseudo-continuous models.

The model parameters were estimated by fitting a considerable amount of experimental data covering a wide range of aspect ratios ( $a = 5.6 - \infty$ ). These parameters have a clear physical meaning, as they define the spatial location and density of the particle centres. Those fixing the position of particle centres were found to be practically independent of the aspect ratio of the bed, while the number of particle centres in each zone was expressed in terms of a compact arrangement of particles, producing a theoretical dependence on  $a$ .

For  $2 < a < 5.6$ , the experimental information is very scarce. An experimental voidage profile for  $a = 3.96$  could be well fitted to the model while employing a different set of values for the parameters. Thus, the approach followed in this study is likeliest to be useful in this range of  $a$ , and more experimental data are needed to reach predictive capabilities.

Finally, it is worth noting that real spherical packing will usually present some dispersion in particle size. These cases are

much less systematically studied, and further effort is needed to obtain predictive expressions. The formulation presented here could be readily extended by assembling the contribution of particles in each size class.

## Acknowledgements

The authors wish to thank the financial support of the following argentine institutions: ANPCyT-SECyT (PICT N# 00227 and N# 06297), CONICET (PIP96 N# 4791) and UNLP (PID N# 11/I058). O.M.M. and G.F.B. are Research Members of the CONICET and N.J.M. is a fellow of the CONICET.

## Nomenclature

$a$	aspect ratio, ( $d_T/d_p$ )
$d_p$	particle diameter, (m)
$d_T$	vessel or tube diameter, (m)
$N_c$	number of particles per unit bed length in a compact arrangement, ( $m^{-1}$ )
$N_p$	total number of particles per unit bed length, ( $m^{-1}$ )
$N_{pj}$	number of particle centres per unit bed length in the $j^{\text{th}}$ zone, ( $m^{-1}$ )
$r$	radial coordinate, (m)
$r_c$	radial position of the particle centre, (m)
$R_p$	particle radius, (m)
$R_T$	vessel tube radius, (m)
$S(\xi, \mu)$	area of a cylindrical surface intersected by a sphere, ( $m^2$ )
$V(\xi, \mu)$	volume of a sphere intersected by cylindrical surface, ( $m^3$ )
$x$	dimensionless distance from the wall, $(R_T-r)/d_p$
$x_{min}$	value of $x$ corresponding to the first stationary minimum voidage

## Greek Symbols

$\bar{\epsilon}$	overall bed voidage
$\rho(r)$	radial voidage
$\rho(r_c)$	radial density function of particle centres, ( $m^{-3}$ )
$\rho_j$	contribution of the $j^{\text{th}}$ zone to $\rho(r_c)$ , ( $m^{-3}$ )
$\bar{\rho}_j$	average number of particle centres in the $j^{\text{th}}$ zone, ( $m^{-3}$ )

## References

- Benenatti R.F. and C.B. Brosilov, "Void Fraction Distribution in Bed of Spheres", *AIChE J.* **8** (3), 359–361 (1962).
- Delmas, H. and G.F. Froment, "A Simulation Model Accounting for Structural Radial Nonuniformities in Fixed Bed Reactors", *Chem. Eng. Sci.* **43**, 2281–2287 (1988).
- Giese, M., K. Rottschäfer and D. Vortmeyer, "Measured and Modelled Superficial Flow Profiles in Packed Beds with Liquid Flow", *AIChE J.* **44**, 484–490 (1998).
- Goodling, J.S., R.I. Vachon, W.S. Stelpflug and S.J. Ying, "Radial Porosity in Cylindrical Beds Packed with Spheres", *Powder Techn.* **35**, 23–29 (1983).
- Govindarao, V.M.H. and G.F. Froment, "Voidage Profile in Packed Beds of Spheres", *Chem. Eng. Sci.* **41**, 533–539 (1986).

- Govindarao, V.M.H. and K.V.S. Ramrao, "Prediction of Location of Particles in the Wall Region of a Randomly Packed Bed of Spheres", *Chem. Eng. Sci.* **43**, 2544–2545 (1988).
- Govindarao, V.M.H., K.V.S. Ramrao and A.V.S. Rao, "Structural Characteristics of Packed Beds of Low Aspect Ratio", *Chem. Eng. Sci.* **47**, 2105–2109 (1992).
- Legawiec, B. and D. Ziolkowski, "Structure, Voidage and Effective Thermal Conductivity of Solids within Near-Wall Region of Beds Packed with Spherical Pellets in Tubes", *Chem. Eng. Sci.* **49**, 2513–2520 (1994).
- Mariani N.J., G.D. Mazza, O.M. Martínez and G.F. Barreto, "Evaluation of Radial Voidage Profile in Packed Beds of Low Aspect Ratios", *Can. J. Chem. Eng.* **78**, 1133–1167 (2000).
- Mariani, N.J., G.D. Mazza, O.M. Martínez and G.F. Barreto, "The Distribution of Particles in Cylindrical Packed Beds", *Trends in Heat, Mass and Momentum Transfer* **4**, 95–114 (1998).
- Mariani, N.J., Martínez O.M. and Barreto G.F., "Computing Radial Packing Properties from the Distribution of Particle Centers", *Chem. Eng. Sci.* **56**, 5693–5707 (2001).
- Mueller, G.E., "Radial Void Fraction Distributions in Randomly Packed Fixed Beds of Uniformly Sized Spheres in Cylindrical Containers", *Powder Techn.* **72**, 269–275 (1992).
- Press, W.H., S.A. Teukolsky, W.T. Vetterling and B.P. Flannery, "Numerical Recipes in Fortran", 2<sup>nd</sup> ed., Cambridge University Press, Cambridge, UK (1992).
- Ridway K. and K.J. Tarbuck, "Radial Voidage Variation in Randomly-Packed Beds of Spheres of Different Sizes", *J. Pharm. Pharmac.* **18**, Suppl., 168S–175S (1966).
- Stewart W.E., M. Caracotsios and J.P. Sorensen, "Parameter Estimation from Multiresponse Data", *AIChE J.* **38** (5), 641–650 (1992).
- Winterberg M., E. Tsotsas, A. Krischke and D. Vortmeyer, "A Simple and Coherent Set of Coefficients for Modelling of Heat and Mass Transport with and without Chemical Reaction in Tubes Filled with Spheres", *Chem. Eng. Sci.* **55**, 967–979 (2000).

Manuscript received January 11, 2001; revised manuscript received November 23, 2001; accepted for publication January 24, 2002.